ELSEVIER

Journal of Photochemistry and Photobiology A: Chemistry 154 (2003) 131–144

Journal of Photochemistry and Photobiology A:Chemistry

www.elsevier.com/locate/jphotochem

Steric substituent effects of new photochromic tetrahydroindolizines leading to tunable photophysical behavior of the colored betaines

Saleh A. Ahmed [a,*], Aboeł-Magd A. Abdel-Wahab [a], Heinz Dürr [b]

[a] *Chemistry Department, Faculty of Science, Assiut University, 71516 Assiut, Egypt*
[b] *Fachrichtung 11.2, Organische Chemie, Universität des Saarlandes, D-66041 Saarbrücken, Germany*

Received 9 May 2002; received in revised form 16 July 2002; accepted 29 August 2002

Dedicated to Prof. Dr. H. Bouas-Laurent on the occasion of his retirement

Abstract

Various substituted photochromic tetrahydroindolizine (THIs) derivatives **4a–r** have been synthesized by nucleophilic addition of 1-phenyl-3,4-dihydroisoquinolines **2** to spirocyclopropene **1**. After irradiation of the THIs **4a–r** with UV light, a blue to green colored zwitterionic betaines **3a–r** was formed which undergoes a thermal electrocyclization leading to colorless THIs **4a–r**. Both the half-life of the thermal back reaction and the absorption spectra of the colored forms are found to be strongly dependent on the position and size of the substituent in the 10′b-phenyl ring. A strong pronounced effect was observed by comparison of each *ortho*-substituents to the corresponding *para*-substituents which showed increase in the half-life by a factor of 4 for *o*-, *p*-fluoro-substitution **3h–j** and a factor of 2000 for *o*-, *p*-iodo-substitution **3q**,**r**. *Meta*- and *para*-substitution showed no pronounced influence on the half-life. The steric effect of different groups was well proved by CHARMm calculation. The computational results provided a new insight into the reaction pathway signifying the steric effect of substituents on THIs **4**. The energies of the unsubstituted THI **4a**, the *ortho*-substituted THIs **4b**,**e**,**k** and the *meta*-derivatives **4c**,**f**,**l** as well as their betaines for the *cisoid* **3**″ and *transoid* **3**‴ were studied. The structures and energies for **3b**,**e**,**k**,**c**,**f**,**l** were monitored. In conclusion, the formation of the twisted open form **3**′ is responsible for value of the rate constant of the thermal cyclization.

Keywords: Photochromism; Tetrahydroindolizines; Betaines; Steric hindrance; CHARMm calculations

1. Introduction

Photochromism, one of the most striking phenomena of photochemistry, which involves light-induced reversible transformation of a molecule between two states with different distinguishable absorption spectra, has received great attention in the recent years [1–5]. Reversible coloration and bleaching upon wavelength-controlled illumination are very desirable characteristics for inks and dyes, biological sensors, optical switches [6,7]. Additionally, such organic photochromic materials could be used in rewritable optical memories, as media for high capacity and ultrafast computing storage devices [6–9]. Currently, the bottleneck, restraining the potential use of such devices, is the synthesis of suitable materials [10], which require indispensable properties such as the thermal stability of both isomers as well as high fatigue resistance [11,12].

Amongst the many photochromic systems, which reversibly inter-converted between distinct forms by irradiation, photochromic tetrahydroindolizines (THIs), which discovered and developed in the laboratories of H. Dürr in 1979, had received particular attention owing to their remarkable photofatigue-resistance and wide broad photochromic properties [13–17]. The characteristic photophysical data of the photochromic THI are strongly influenced by the electronic and steric effects of the substituents [13–17]. Previous work on the photochromic tetrahydroindolizines has focused only on introducing various groups with electron donating or withdrawing character, whilst the steric effect was often neglected [13–16].

In continuation of our work dealing with the preparation and study of the photophysical properties of photochromic THIs, this paper will shed more light on the effect of different groups on the photophysical behavior of new photochromic THIs and to control the changeability of the position of the band maxima in the absorption spectra and

* Corresponding author. Present address: Special Division for Human Life Technology, National Research Institute of Advanced Industrial Science and Technology (AIST), 1-8-31 Midorigaoka, Ikeda, Osaka 563-8577, Japan. Fax: +2088312564.
E-mail address: saleh_63@hotmail.com (S.A. Ahmed).

1010-6030/03/$ – see front matter
PII: S1010-6030(02)00327-1

half-life of tetrahydroindolizines (THIs) **4a–r** and betaines **3a–r** by modifying the position of the substituents (*o*-, *m*-, and *p*-) of the phenyl group in the 10′b-position of tetrahydroindolizines THIs **4a–r**. The molecular modeling calculations as well as X-ray crystallographic analysis are highly effective methods which clearly assigned the steric hindrance of different substituents in the 10′b-phenyl ring which lead to new insights into the mechanism of electrocyclization of the betaines **3a–r** ↔ **4a–r**.

2. Experimental

All studied THIs **4a–r** were prepared according to literature procedure [17]. Characterization of the chemical structures was achieved using both analytical and spectroscopic measurements. The ^{1}H NMR spectra were recorded at 500 MHz spectrometer using tetramethylsilane as internal standard. Chemical shifts are reported in δ (ppm) and coupling constants in Hertz (Hz). The UV/Vis absorption spectra were recorded in dichloromethane. The time resolved spectra of fast bleaching THI were determined by flash photolysis. Dichlormethane (spectrophotometric grade) was used as received. Mass spectra were obtained using FAB mode. Elemental analyses were carried out with a CHNS-analysator.

The molecular modeling was carried out using "CHARMm calculations". The structures have been calculated using Quanta Release 4.0 Version 94.0222-CHARMm on a workstation. Computations were done in the gas phase. The positive and negative charge was locked and the "Gasteiger method" was applied. Minimization was executed with "conjugate gradient" until the difference of energy between two calculation steps was zero. Experimental details and full characterizations of these new photochromic THIs will be published elsewhere [17].

3. Results and discussion

The effect of substituents with different mesomeric (M-) and inductive (I-) effects on the photochromism of dihydroindolizines (DHIs) is well known and can be analyzed by Hammett-correlation [14–16]. For example, the attachment of electron-withdrawing groups (positive σ-values) to the heterocylic moiety (region **C**) [14–16] of the DHI molecules leads to an increase of the rate constant (*k*; positive σ-values) of the thermal back electrocyclization (betaine → DHI, Fig. 1).

To study the steric effect of different subsitutents on the 10′b-phenyl ring of THIs **4a–r**, we have successfully changed the position of different substituents of the phenyl ring in the 10′b-position of THIs **4** (Fig. 2). New tetrahydroindolizines (THIs) **4** bearing nitro- and methyl-groups as well as halogen atoms in different positions of the 10′b-phenyl ring were synthesized [17].

Substituted 1-phenyl-3,4-dihydroisoquinolines **2a–r** were prepared by modification of the Bischler–Napieraski [18,19] reaction. The nucleophillic addition of substituted-3,4-dihydroisoquinolines **2a–r** to spirocyclopropene **1** afforded the THIs **4a–r** after purification by column chromatography on silica gel in moderate to good yields (33–94%) [17]. NMR, IR, mass spectrometry and elemental analysis characterized all synthesized THIs **4a–r** [17].

The chemical structure of photochromic diisopropyl 5′,6′-dihydro-10′b-(2-iodophenyl)-1′H-spiro[fluorene-9,1′-pyrrolo[2,1-a]isoquinoline-2′,3′-dicarboxylate **4q** was confirmed by X-ray single crystal analysis (Fig. 3). All the THI regions **A**, **B**, **C** [1] as fluorene, ester and dihydroisoquinoline parts are clearly assigned [17].

The single crystal of the new THI **4q** (Fig. 3) was successfully prepared [17] (with crystal size 0.4 mm × 0.3 mm × 0.28 mm in CH_2Cl_2/*n*-pentane (v/v; 1:2) after standing at room temperature for several days. The crystal system was monoclinic, space group was P2(1)*c* and unit cell dimensions are: (a = 11.305 Å, b = 15.455 Å, c = 18.520 Å, α = 90°, β = 92.57°, δ = 90°). The X-ray diffraction analysis showed that the crystal has empirical formula ($C_{38}H_{34}INO_4$) and molecular weight of 695.56.

The bond length values showed that, there is a single bond between C(4)–C(5), C(1)–C(12) and a double bond between C(2)–C(35). The bond lengths in the annulated benzene and 10′b-phenyl rings are consistent with characters [20]. The single bonds between C(12)–C(11), C(12)–C(13), C(6)–C(5), C(1)–C(2), C(1)–C(30), C(1)–C(19), C(24)–C(25), N(1)–C(3), N(1)–C(4) and N(1)–N(12) showed similar values when compared with standard bond lengths [21–23]. Due to the tension in the region of dihydropyrrole

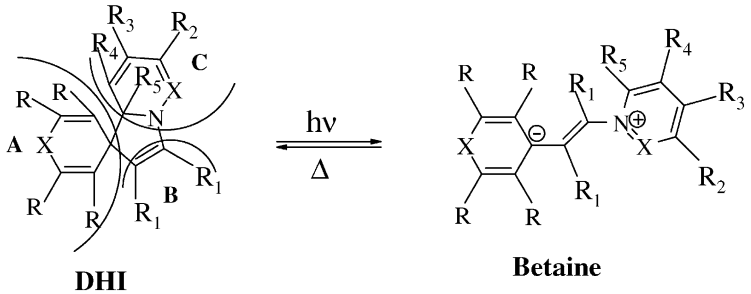

Fig. 1. Schematic representation of the light-induced ring opening of the DHI (the three regions **A**, **B**, **C** are represented) to the corresponding colored betaine.

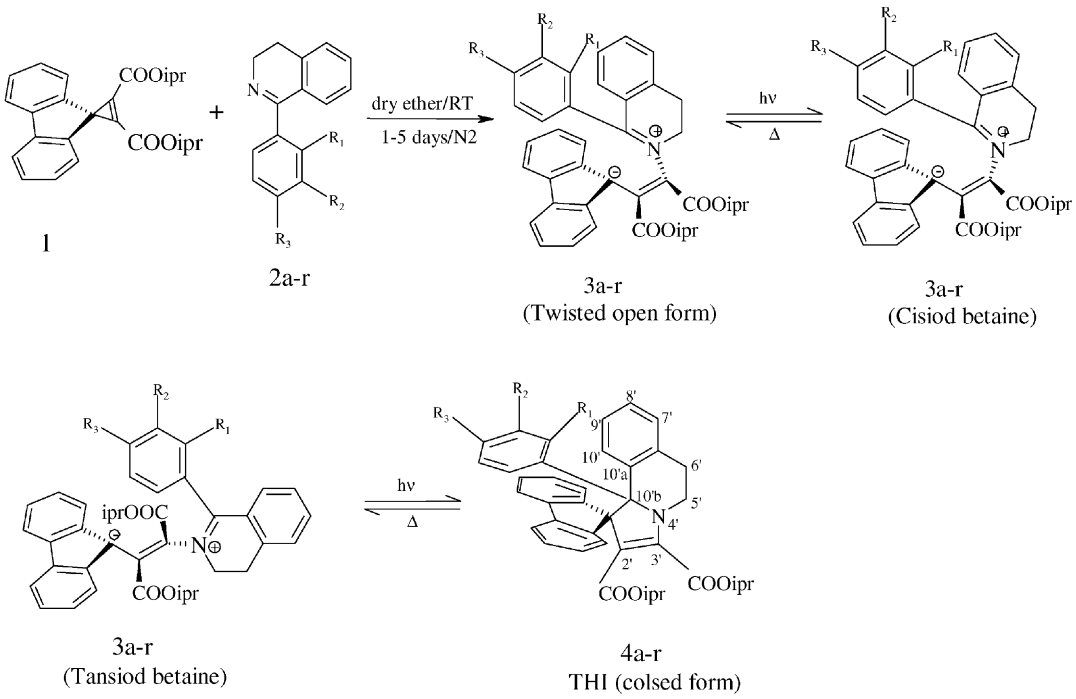

Fig. 2. Preparation of new photochromic tetrahydroindolizines **4a–r** and proposed structures for the successive betaine forms **3a–r** appearing after light-induced ring opening of the spiro THIs **4**.

ring, the bond lengths between N(1)–C(12) (1.502 Å) and C(1)–C(12) (1.613 Å) are longer than the corresponding standard bond lengths (1.470 and 1.540 Å). This lengthening of the single bonds may be due to the spiro-concatenation on C(1). This was also shown by MINDO/3-calculation in the spiro–azanonatriene system [22,23]. On the other hand, the longer bond length of C(1)–C(12) of **4q** (1.613 Å) makes it relatively weak and easily cleaved upon irradiation with UV light leading to ring opened betaine **3q** [17,23].

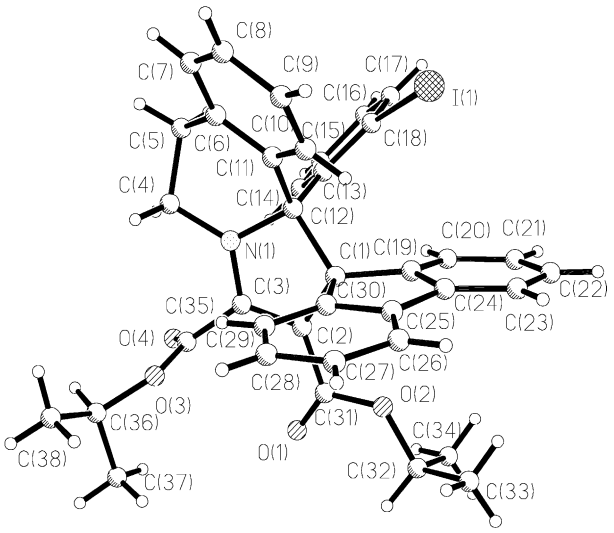

Fig. 3. X-ray crystal structure of THI **4q**.

The bonds and dihedral angles of C1–C2–C3–N1 showed clearly that the dihydropyrrole-[2,1-a]-dihydroisoquinoline region is not planar and that the nitrogen atom N(1) and the center C(1) lie out of plane. C(2), C(3) and N(1) atoms are sp^2-hybridized since a summation of the bond angles being approximately 360° [23]. Another interesting aspect of the molecule that could be observed from the X-ray analysis is that the 10′b-(*o*-iodophenyl) ring lies under both the fluorene core and dihydroisoquinoline moiety. This could be attributed to the steric effect of the bulky substituent such as iodine can cause significant steric effect. Such steric effect plays a key role upon the flourene and isoquinoline skeleton of the molecule, which undergo slow electrocylization to THI **4q** thermally. Further X-ray crystallographic data are listed as supplementary material.

*3.1. Photochromism of THIs **4a–r** and their corresponding betaines **3a–r***

*3.1.1. Influence of substituents on the absorption spectra of THIs **4a–r***

All THIs **4a–r** are colorless in the solid state or in dichloromethane (λ_{max} between 320 and 332 nm) except for the 10′b-nitro substituted THIs **4b–d** which has a yellow color (λ_{max} between 340 and 356 nm) (Fig. 4 and Table 1). The molar absorptivity (ε) varies between 8050 (**4a)** and 18,390 $mol^{-1}\,dm^3\,cm^{-1}$ (**4l)**. The presence of the substituents does not greatly influence the energy of the absorption maximum. However, the molar absorptivity increases

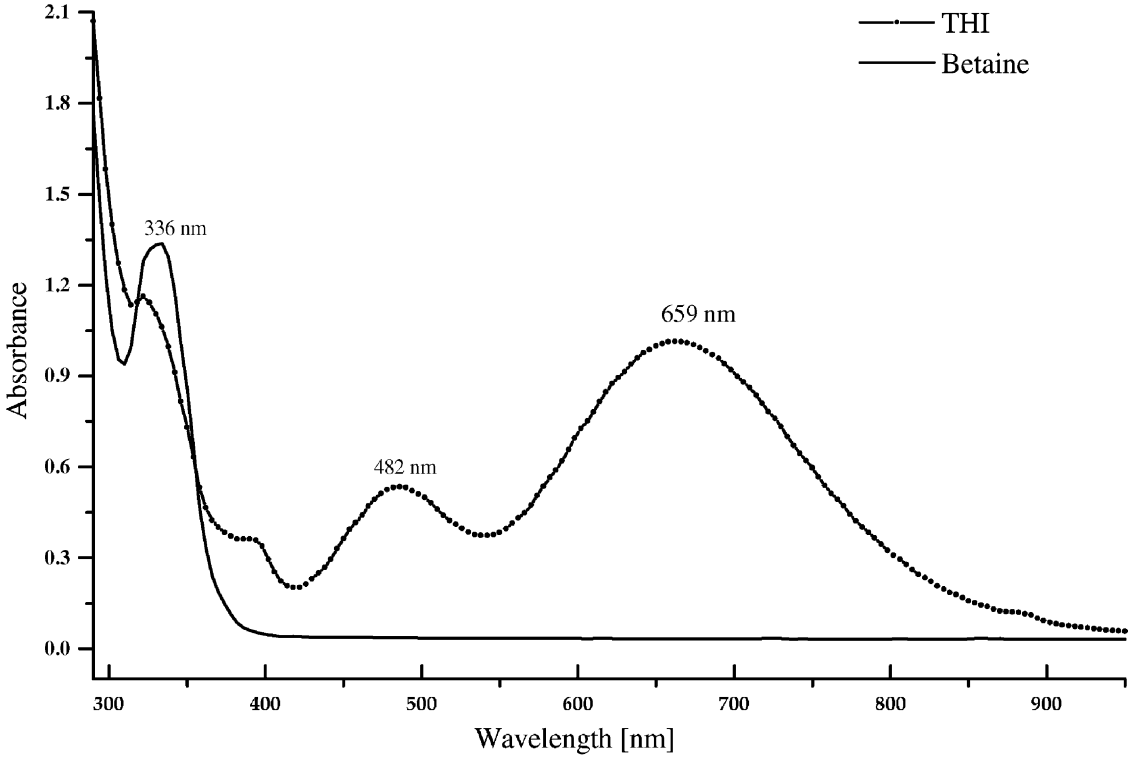

Fig. 4. UV-Vis spectrum of THI **4q** and the corresponding betaine **3q** in dichloromethane ($c = 2 \times 10^{-4}$ mol l^{-1}) at ambient temperature.

with the introduction of different group positions. Substitutions of different groups in *meta*- and *para*-positions have approximately the same molar absorpativity. Substitutions in the *ortho*-position have a 20% lower ε value than that of the *meta*- and *para*-substituted derivatives.

Table 1
UV-data and half-life time of THIs **4a–r** and betaines **3a–r** in dichloromethane ($c = 2 \times 10^{-4}$ mol l^{-1}) at ambient temperature

3/4	λ_{max} THI (nm)	λ_{max} Betaine (nm)	$t_{1/2}$ (s)	Color of betaine
a (H)	327	480, 719	16.47	Green
b (*o*-NO_2)	340	485, 690	484.7	Green-blue
c (*m*-NO_2)	342	500, 700	2.6	Green
d (*p*-NO_2)	356	450, 702	0.96	Green
e (*o*-Me)	332	481, 686	2052.67	Green-blue
f (*m*-Me)	321	480, 712	5.81	Green
g (*p*-Me)	320	480, 722	18.89	Green
h (*o*-F)	325	480, 683	47.96	Green-blue
i (*m*-F)	324	480, 711	7.44	Green
j (*p*-F)	330	470, 700	11.18	Green
k (*o*-Cl)	328	480, 668	1851.80	Blue
l (*m*-Cl)	326	482, 705	3.67	Green
m (*p*-Cl)	325	480, 710	16.24	Green
n (*o*-Br)	325	484, 659	5351.66	Blue
o (*m*-Br)	323	480, 714	4.48	Green
p (*p*-Br)	320	480, 720	6.85	Green
q (*o*-I)	336	482, 659	14663.58	Blue
r (*p*-I)	322	481, 721	7.39	Green

*3.1.2. Influence of substituents on the photochromic behavior of betaines **3a–r***

Irradiation of THIs **4a–r** with polychromatic light leads to ring opening betaines **3a–r** (Fig. 2), which absorb in the visible region (between 450 and 722 nm). The UV-spectra of the colored betaines **3a–r** exhibit two absorption maxima; between 450 and 500 nm and 659 and 722 nm (Fig. 4). The color of betaines varied from blue to green, which is strongly depending on the type and position of the substitution in the 10′b-phenyl ring (Table 1). The second absorption maxima (659 and 722 nm) of betaines **3** are strongly affected by the substitution in *ortho*, *meta* or *para* positions (Figs. 5–10). The effect of substitution in the 10′b-phenyl ring on the UV-absorption of the betaines showed that the substitution in the *ortho*-position (Figs. 6 and 8) leads to a hypsochromic shift compared with the *meta*- and *para*-substituted species (Figs. 7, 9 and 10). This is mainly attributed to the steric effect of the substituents in the *ortho*-position of 10′b-phenyl ring of the THI molecule. In generally, this phenomenon has been considered that a bulky substituent sometimes causes strain to hamper charge delocalization, namely, planar structure formation resulted in hypsochromic shift.

Minimal shift differences were observed when the strong electron attracting nitro groups were placed in either the *ortho*, *meta* or *para* position of the 10′b-phenyl ring. On the other hand, the maximum hypsochromic shift was observed in the case of *ortho*-substituted bromine and iodine betaines **3n**,**q** (60 nm, Fig. 6) compared with the unsubstituted

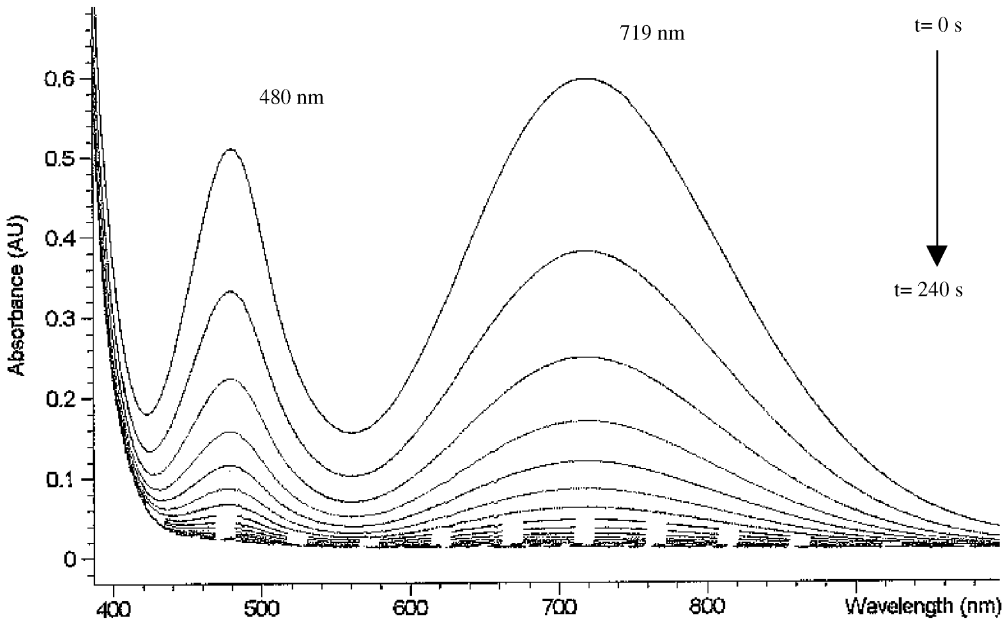

Fig. 5. Kinetic UV-Vis spectrum of the thermal fading of betaine **3a** to THI **4a** (cycle time = 10 s, run time = 240 s) in CH_2Cl_2 ($c = 2 \times 10^{-4}$ mol l^{-1} at 296 K).

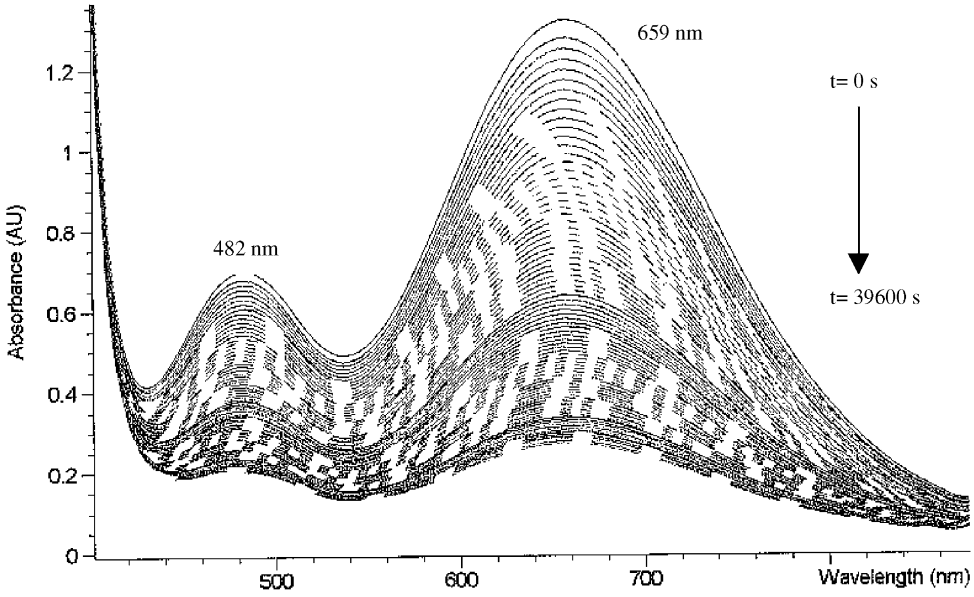

Fig. 6. Kinetic UV-Vis spectrum of the thermal fading of betaine **3q** to THI **4q** (cycle time = 480 s, run time = 39,600 s) in CH_2Cl_2 ($c = 2 \times 10^{-4}$ mol l^{-1} at 296 K).

betaine **3a** (Fig. 5). Changing the electronic influence from electron withdrawing to electron donating groups causes also hypsochromic shift (Table 1). A comparison of various *ortho*-substituted betaines **3b**,**e**,**h**,**k**,**n**,**q** show a decrease of λ_{max} by 31 nm from *o*-nitro **3b** to *o*-iodo **3q** (Figs. 6 and 8). This may due to both electronic and steric effects [17].

3.1.3. Influence of substituents on the half-life of the 1,5-electrocyclization

The kinetic of thermally induced ring closure of betaines **3a–r** was measured at 25 °C in dichloromethane [17]. As expected, the introduction of electron-withdrawing groups in the *meta*- and *para*-positions of the 10′b-phenyl ring destabilizes the positively charged heterocyclic part (region **C**) [1] of the betaines. This effect decreases the half-life of the substituted betaines compared to the unsubstituted betaine **3a** (16.47s) (Fig. 11). The +*I*-effect of methyl group at *para*-position, however, has the opposite effect to increase the half-lives (18.89s).

It is observed that the electrocyclization of 10′b-(*o*-substituted phenyl)betaines **3b**,**e**,**h**,**k**,**n**,**q** are generally slower by a factor of 3 (as shown in **3h**) to 900 (**3q**) (Figs. 8 and 12) when

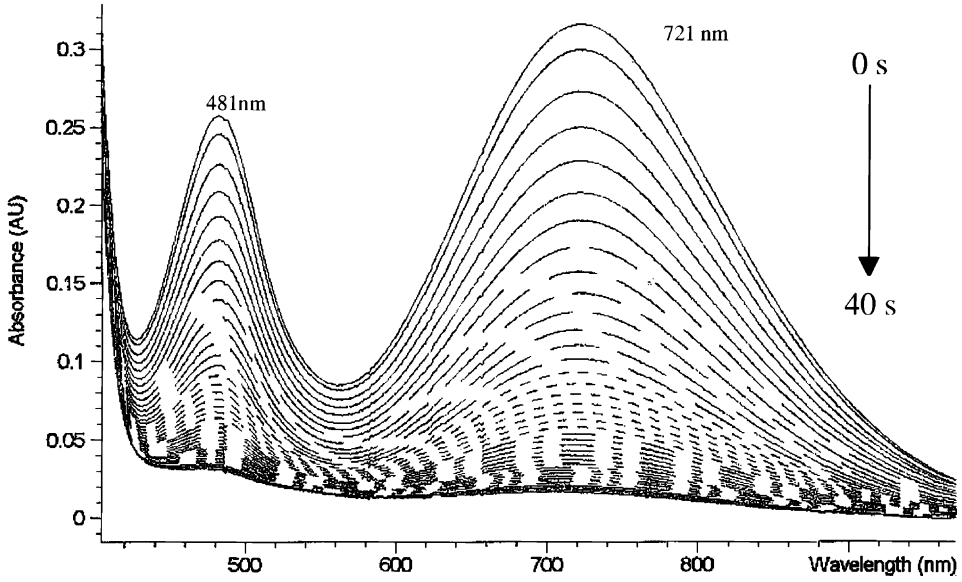

Fig. 7. Kinetic UV-Vis spectrum of the thermal fading of betaine **3r** to THI **4r** (cycle time = 1 s, run time = 40 s) in CH_2Cl_2 ($c = 2 \times 10^{-4}$ mol l^{-1} at 296 K).

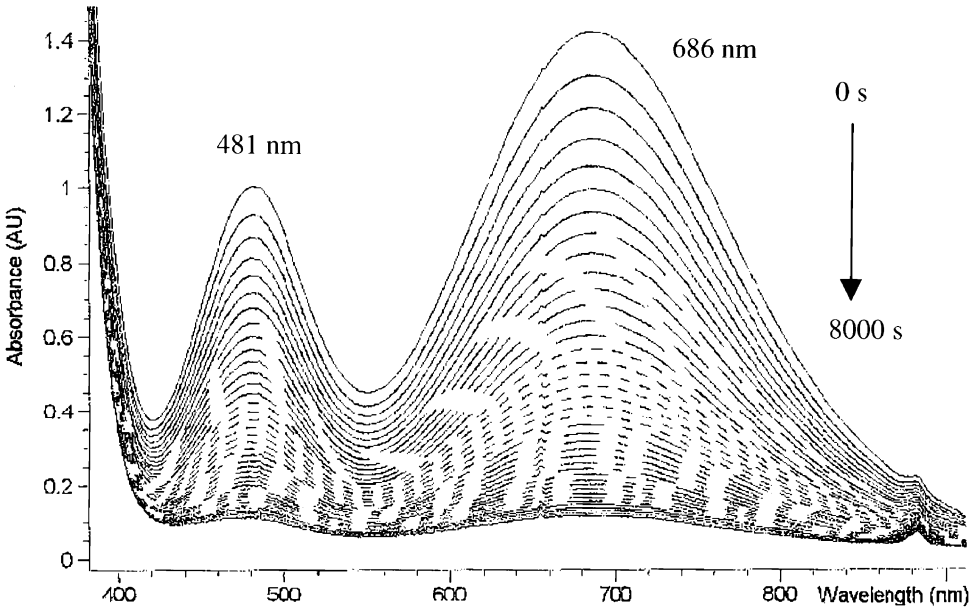

Fig. 8. Kinetic UV-Vis spectrum of the thermal fading of betaine **3e** to THI **4e** (cycle time = 200 s, run time = 8000 s) in CH_2Cl_2 ($c = 2 \times 10^{-4}$ mol l^{-1} at 296 K).

compared to the electrocyclization of the parent betaine **3a** (Fig. 11). A comparison of each *ortho*-substituent to the corresponding *para*-substituent showed an increase by a factor of 505 for *o*-, *p*-nitro substitutions **3h–j** and a factor of 2000 for *o*-, *p*-iodo substitutions **3q**,**r** (Figs. 12–16). *Meta*- and *para*-substitutions showed no pronounced influence on the half-life (Figs. 11, 13, 15 and 16). This clearly indicates an influence of the *ortho*-steric effect in hindering the thermal 1,5-electrocyclization [17,23–25]. A comparatively small *ortho* effect on the thermal 1,5-electrocyclization can be found in the fluorine substituted betaines **3h**,**j** (47.96s and 11.18s, respectively) that is due to its small atomic size. In addition to the X-ray analysis (Fig. 3), molecular modeling calculations using CHARMm calculations has been performed to study these strong *ortho*-substitutent effects on both half-lives and absorption maxima of colored betaines **3**.

*3.2. Molecular modeling by CHARMm calculations for selected THIs **4a–r** and their corresponding betaines **3a–r***

The equilibrium between reactants and the transition state, like other equilibria, is affected by the repulsions between

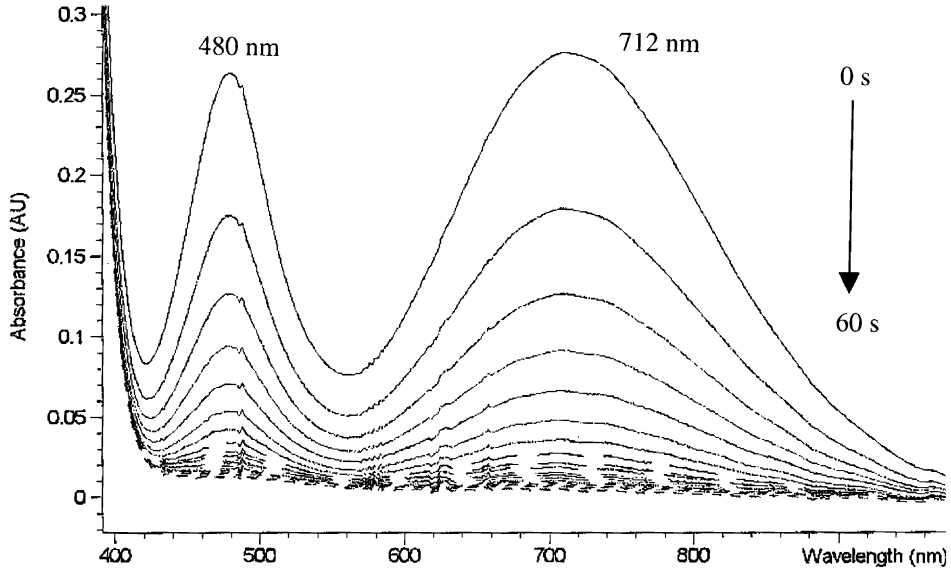

Fig. 9. Kinetic UV-Vis spectrum of the thermal fading of betaine **3f** to THI **4f** (cycle time = 3 s, run time = 60 s) in CH_2Cl_2 ($c = 2 \times 10^{-4}$ mol l^{-1} at 296 K).

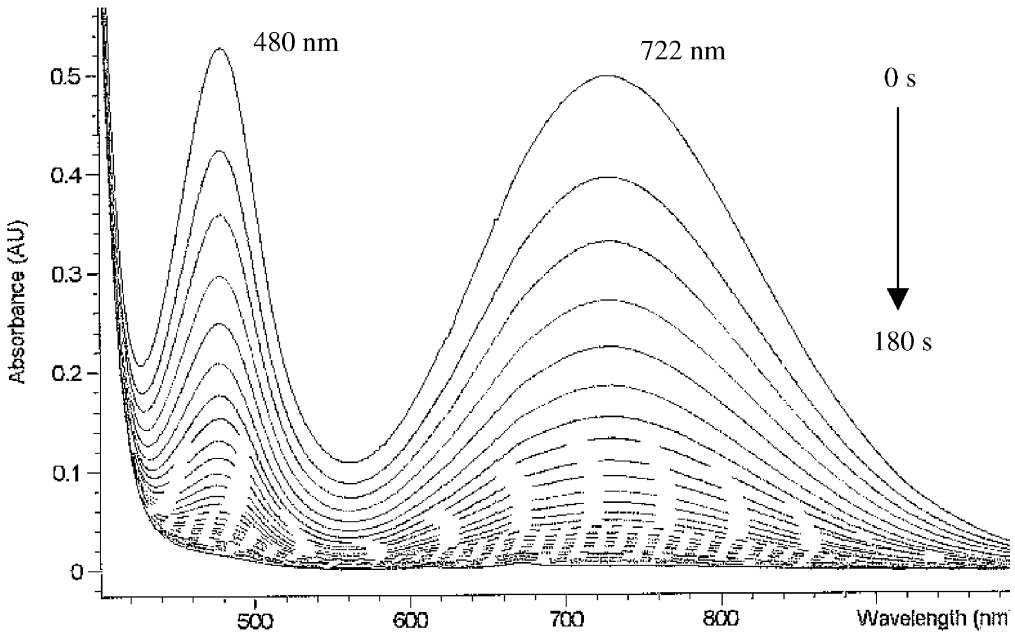

Fig. 10. Kinetic UV-Vis spectrum of the thermal fading of betaine **3g** to THI **4g** (cycle time = 5 s, run time = 180 s) in CH_2Cl_2 ($c = 2 \times 10^{-4}$ mol l^{-1} at 296 K).

atoms that are brought near to each other as a result of the steric requirements of bond distances and angles. When these repulsions serve to increase the free energy of the reactants more than that of the transition state, these steric requirements increase the reaction rate, and the reverse case causes the reaction to be retarded [25b]. The steric factor acts in various ways. The simple repulsion between groups can be different in two systems. The steric factor can impose a configuration in which the directly transmitted effects of the polarities of substituents groups are either at a maximum or at a minimum. The repulsions between groups can interfere with configurations favorable to resonance. The steric factor also determines the formation of the chelate rings. However, steric effects can result in an increase as well as a decrease of the reaction rates (k). Substitution in *ortho*-position is one of the most common causes of steric effects [24b]. The earliest observation of the steric effect of *ortho*-groups was made by Hofmann [27], who found that dimethylanilines with both *ortho*-positions occupied by quaternary salts reacts very slowly when heated with methyl iodide at 150 °C. The

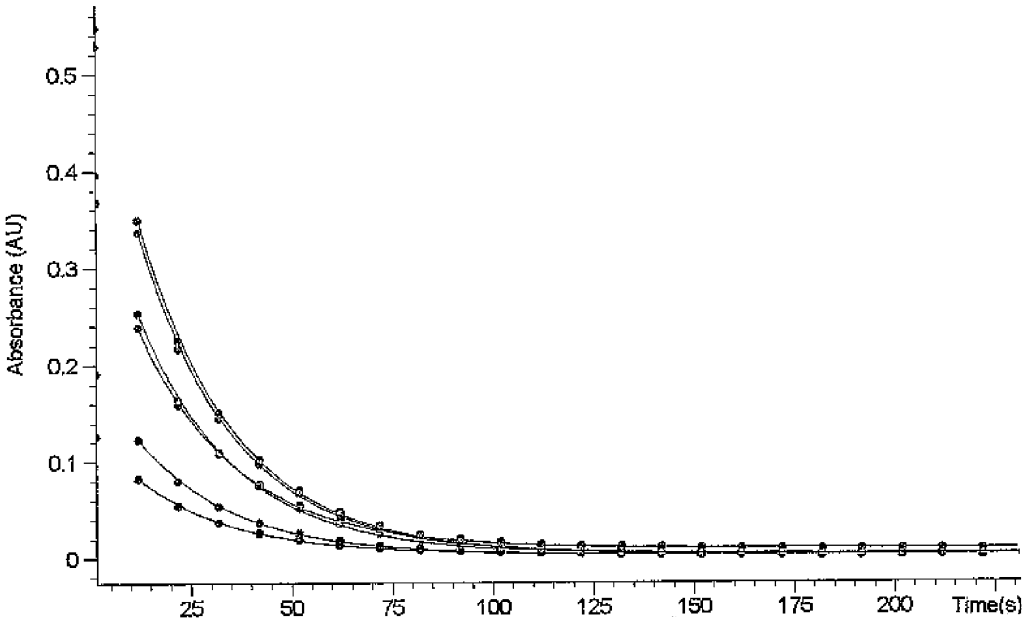

Fig. 11. Absorbance–time relationship for the kinetic thermal fading of betaine **3a** at different wavelengths for determination of the electrocyclization rate constant k (500 nm, $k = 4.14 \times 10^{-2}\,s^{-1}$; 550 nm, $k = 4.21 \times 10^{-2}\,s^{-1}$; 600 nm, $k = 4.21 \times 10^{-2}\,s^{-1}$; 650 nm, $k = 4.21 \times 10^{-2}\,s^{-1}$; 700 nm, $k = 4.21 \times 10^{-2}\,s^{-1}$; and 750 nm, $k = 4.22 \times 10^{-2}\,s^{-1}$ at 296 K).

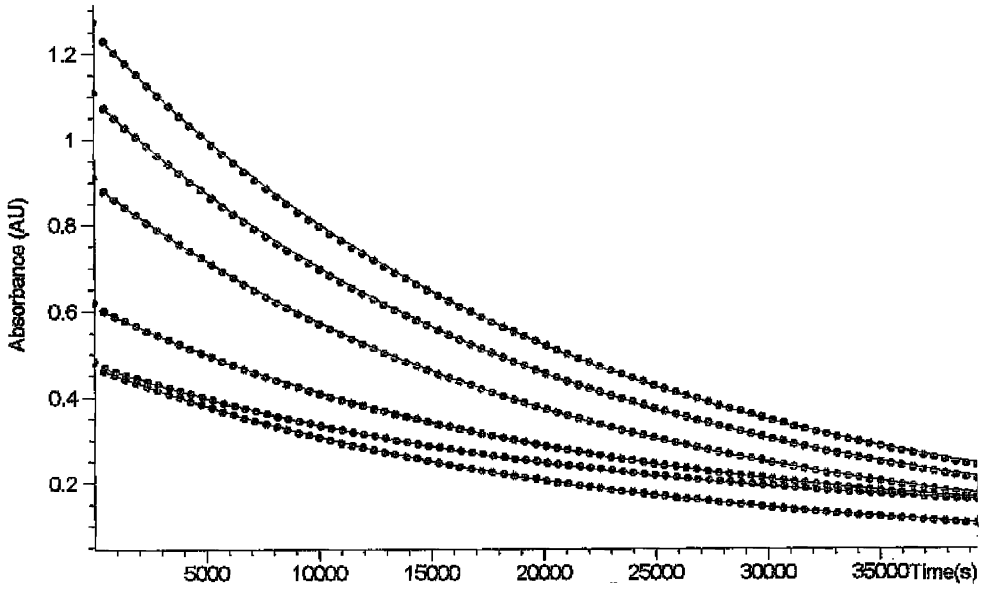

Fig. 12. Absorbance–time relationship for the kinetic thermal fading of betaine **3q** at different wavelengths for determination of the electrocyclization rate constant k (450 nm, $k = 4.74 \times 10^{-5}\,s^{-1}$; 500 nm, $k = 1.73 \times 10^{-5}\,s^{-1}$; 550 nm, $k = 4.73 \times 10^{-5}\,s^{-1}$; 600 nm, $k = 4.72 \times 10^{-5}\,s^{-1}$; 650 nm, $k = 4.72 \times 10^{-5}\,s^{-1}$ and 700 nm, $k = 4.72 \times 10^{-5}\,s^{-1}$ at 296 K).

steric effect of the different groups of selected THIs **4** and their corresponding betaines **3** was analyzed by CHARMm calculations (Fig. 17).

After irradiation of the THIs **4**, a very short-lived intermediate, the twisted open form **3′**, with a lifetime of approximately 1 ns was formed [28]. In this form the two carbon atoms that undergo light induced bond cleavage are sp^3-hybridized. The transformation of these sp^3-hybridized to sp^2 C-atoms leads to the *cisoid*-betaine **3″**. After rotation, the *transoid* betaine **3‴** is formed. The electrocyclization from the *trans*-betaine **3‴** to the ring-closed THIs **4** is considered to pass through the same intermediates. In order to determine the steric effect of the substituents on the thermal back reaction, the transients of the electrocyclic process of the new THIs **4** were analyzed by CHARMm calculations. As an example, the unsubstituted THI **4a** and

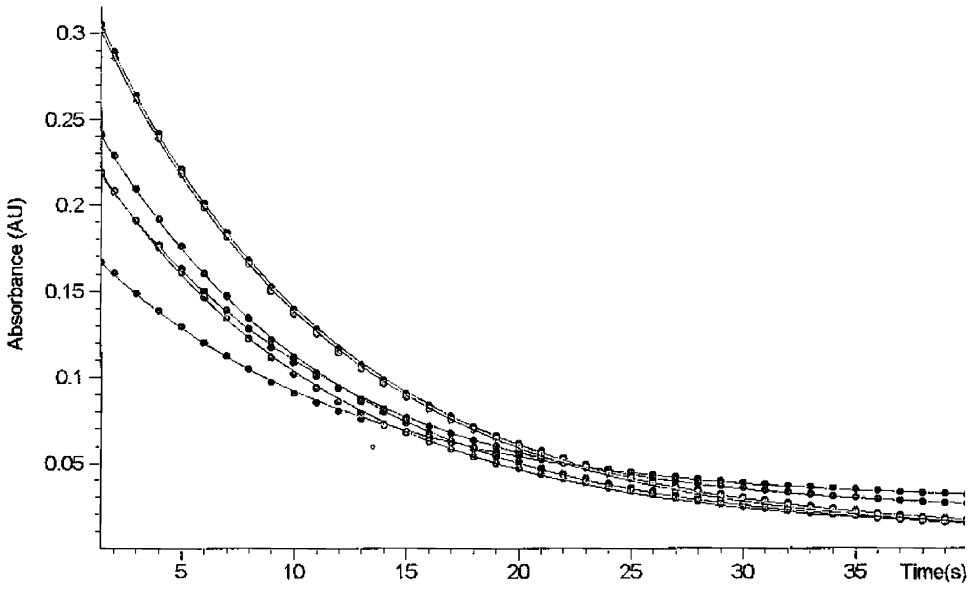

Fig. 13. Absorbance–time relationship for the kinetic thermal fading of betaine **3r** at different wavelengths for determination of the electrocyclization rate constant k (450 nm, $k = 8.88 \times 10^{-2}\,s^{-1}$; 500 nm, $k = 9.17 \times 10^{-2}\,s^{-1}$; 550 nm, $k = 9.33 \times 10^{-2}\,s^{-1}$; 650 nm, $k = 9.32 \times 10^{-2}\,s^{-1}$ and 700 nm, $k = 9.38 \times 10^{-2}\,s^{-1}$; 750 nm, $k = 9.38 \times 10^{-2}\,s^{-1}$ at 296 K).

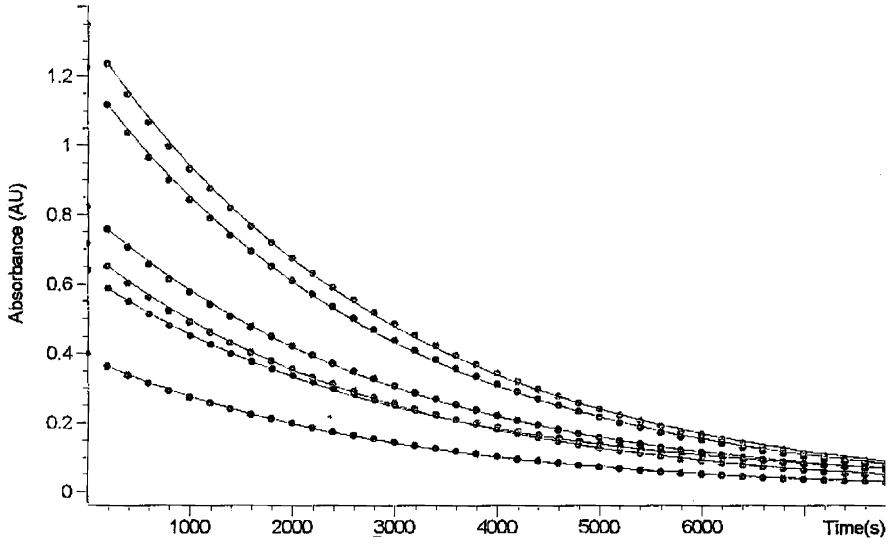

Fig. 14. Absorbance–time relationship for the kinetic thermal fading of betaine **3e** at different wavelengths for determination of the electrocyclization rate constant k (450 nm, $k = 3.63 \times 10^{-4}\,s^{-1}$; 500 nm, $k = 3.33 \times 10^{-4}\,s^{-1}$; 550 nm, $k = 3.42 \times 10^{-4}\,s^{-1}$; 600 nm, $k = 3.41 \times 10^{-4}\,s^{-1}$; 650 nm, $k = 3.77 \times 10^{-4}\,s^{-1}$ and 700 nm, $k = 3.37 \times 10^{-4}\,s^{-1}$ at 296 K).

the *ortho*-substituted THIs **4b**,**e**,**k** and the *meta*-derivatives **4c**,**f**,**l** were studied. For each betaine, *cisoid* **3**″ and *transoid* **3**‴, as well as for the ring-closed THIs **4** the energy minima were determined.

The X-ray structure of a formerly studied stable betaine [23] reveals the kind of bonds existing in the ring-opened structure. The distance of C4–C17 carbon–carbon bond was measured to be 1.351 Å, which is similar to a C–C double bond (ethene: 1.337 Å), whilst the distance between C17–C16 bond is 1.477 Å which is nearly equal to the allyl single bond (1.476 Å). The bond between N15 and C16 is 1.388 Å. This distance reveals that this C–N bond is an intermediate between a single and a double bond (Figs. 17 and 18) [23]. The bond types obtained by the X-ray analysis were used to carry out the CHARMm calculations of the betaines **3**. The C4–C17 and the N15–C16 bond (Fig. 18) were held as double bonds and the bond between C16–C17 was fixed as a single bond. No constraints were set for the calculations of the THIs **4**. For the stability of the THIs **4** the angle θ_1 (C37–C38–C14–N15) is decisive.

Due to the two different positions (*ortho*, and *meta*) of the functional group R (and, thus θ_1) of **3b**,**e**,**k**,**c**,**f**,**l**, two

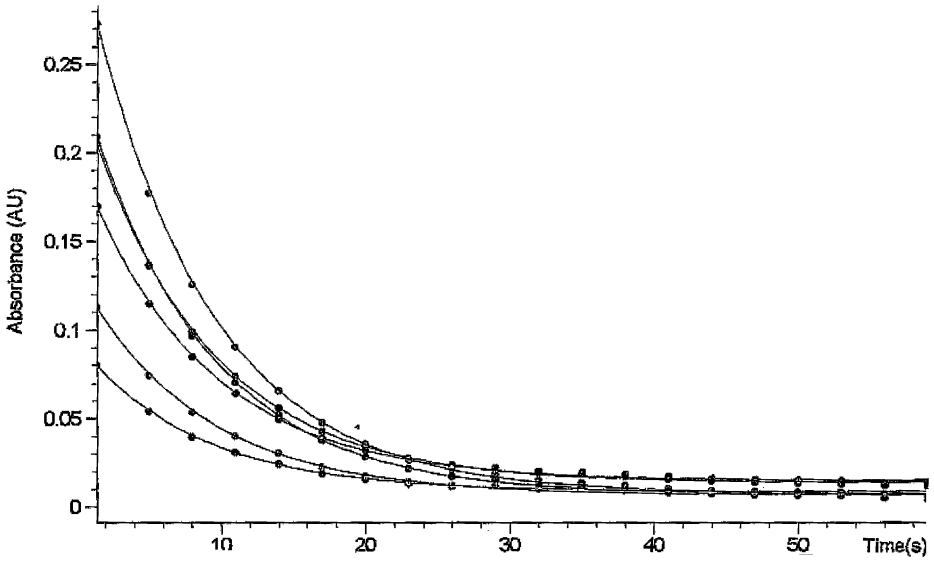

Fig. 15. Absorbance–time relationship for the kinetic thermal fading of betaine **3f** at different wavelengths for determination of the electrocyclization rate constant k (450 nm, $k = 0.12\,s^{-1}$; 500 nm, $k = 0.12\,s^{-1}$; 550 nm, $k = 0.12\,s^{-1}$; 600 nm, $k = 0.12\,s^{-1}$; 650 nm, $k = 0.12\,s^{-1}$ and 700 nm, $k = 0.12\,s^{-1}$ at 296 K).

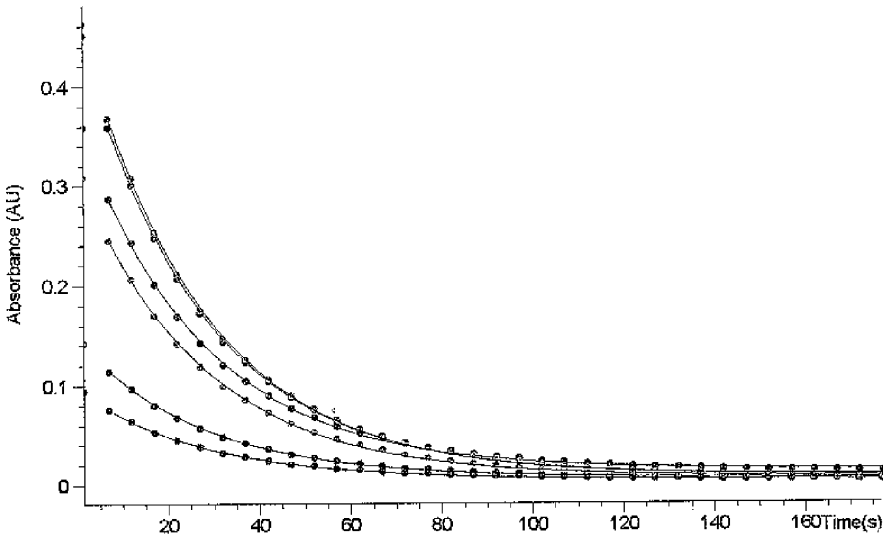

Fig. 16. Absorbance–time relationship for the kinetic thermal fading of betaine **3g** at different wavelengths for determination of the electrocyclization rate constant k (500 nm, $k = 3.67 \times 10^{-2}\,s^{-1}$; 550 nm, $k = 3.70 \times 10^{-2}\,s^{-1}$; 600 nm, $k = 3.67 \times 10^{-2}\,s^{-1}$; 650 nm, $k = 3.70 \times 10^{-2}\,s^{-1}$; 700 nm, $k = 3.72 \times 10^{-2}\,s^{-1}$ and 750 nm, $k = 3.73 \times 10^{-2}\,s^{-1}$) at 296 K.

Table 2
Energy and dihedral angles analysis recorded by CHARMm calculations for THI **4b** and betaine **3b**

4/3	R	Position	Energy	$C_{37}C_{38}C_{14}N_{15}$	$C_{14}N_{15}C_{16}C_{17}$	$N_{15}C_{16}C_{17}C_4$
4b	NO_2	*o*, THI (to ester)	73.6	8.8	–	–
4b	NO_2	*o*, THI (to fluorene)	81.6	169.8	–	–
4b	NO_2	*o*, THI	73.6/81.6	8.8/169.8	–	–
3b	NO_2	*o*, betaine *cisoid*	55.7	60.4	22.7	55.3
3b	NO_2	*o*, betaine *cisoid*	57.7	−119.2	26.0	57.4
3b	NO_2	*o*, betaine *cisoid*	59.5	74.6	−173.0	70.0
3b	NO_2	*o*, betaine *transoid*	59.9	−109.6	179.4	75.9
3b	NO_2	*o*, betaine *transoid*	55.7–59.9	66/−115	24/−176	56/73

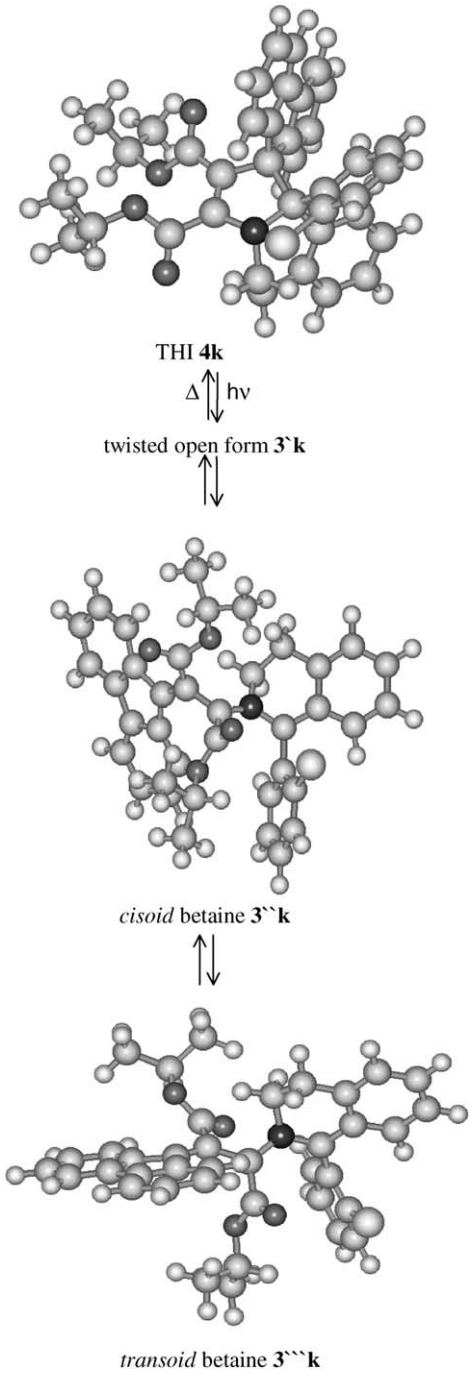

Fig. 17. Mechanistic representation for 1,5-electrocyclization of betaine **3k** to THI **4k** recorded by molecular modeling CHARMm calculations.

structures could be detected. In the first case, the moiety R is directed towards the ester groups and, in the second, towards the fluorene part. Furthermore, CHARMm calculations show that the structures of the betaines are defined by three dihedral angles θ_1–θ_3: θ_1 = C37–C38–C14–N15, θ_2 = *C*14–N15–C16–C17 and θ_3 = *N*15–C16–C17–C4. The *cisoid* **3**″ as well as the *transoid* betaines **3**‴ exhibit four energetic minima characterized by the listed dihedral angles (Tables 2 and 3). The structures and energies of all 65 the

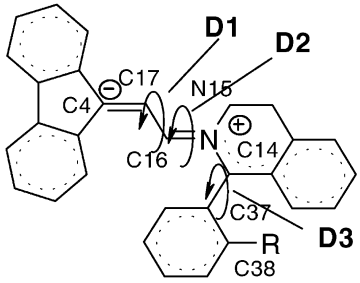

Fig. 18. Representation of bonding nature of betaines **3**.

possibilities for **3b**,**e**,**k**,**c**,**f**,**l** were investigated. The data are collected in the following manner to simplify the overview of the values obtained. The values of the THIs **4**′, the *cisoid* **3**″ and the *transoid* **3**‴ betaines are summarized in a single row. Both energy values of the two THI forms are given separately. The dihedral angles are listed in the same manner. The lowest and highest energy of the betaine structures **3b**,**e**,**k**,**c**,**f**,**l** and the mean values of the dihedral angles are listed in Table 3.

It is observed that the energy of the ring closed form THI **4b** (*ortho*) is higher by 10–15 kJ mol^{-1} than the energy of the corresponding *meta*-substituted THI **4c**. The dihedral angles θ_1 are quite different for all THIs **4** and they are of the orders of 5.2–12.5° and 136.3–169.8°, respectively. The energies of the *ortho*-substituted THIs **4b**,**e**,**k** are clearly higher than the corresponding *meta*- substituted THI **4c**,**f**,**l**. The energy difference between **3e**,**f** and **3k**,**l** was found to be <2 kJ mol^{-1} and the energy difference of about 5–6 kJ mol^{-1} for the nitro substituted betaines **3b**,**c** was calculated. This calculated energy values well indicate that the *transoid* form **3**‴ is more stable than the *cisoid* intermediate **3**″.

The dihedral angle θ_2 of all *cisoid* betaines **3**″ was found to be between 20 and 180° and the dihedral angle θ_3 is 55 or 75° for **3**″. The θ_1 is about 60 and 115°. The θ_1 and θ_2 angles of *cisoid* form **3**″ and the *transoid* betaines **3**‴ are very similar. It is evident that the N15–C16–C17–C4 dihedral angles (θ_3) are completely different from the two ring open forms. The θ_3 angles were observed to be 55 and 74° for the *cisoid* **3**″ and 122 and 131° for the *transoid* form **3**‴. The molecular modeling calculations of the betaines **3** prove that the ring-opened form is rather flexible due to the carbon–carbon bond (C16–C17), which have single bond properties. A steric hindrance for a transition between the *cisoid* **3**″ and *transoid* **3**‴ form was found to be not significant.

The calculated energy for THIs **4** with different substituted groups in the *ortho*- or *meta*-positions show a difference of about 10–15 kJ mol^{-1}. For all *ortho* substituted THIs **4b**,**e**,**k**, a strong steric interaction was found between the R-group, the fluorene part and the ester groups. It can be considered that the twisted open form **3**′, which has nearly the same structure as the ring closed THIs **4**, exhibits the same steric interaction. The facile nature of the transition from **3**‴ to **3**″, the absence of a relation between ease of the transition and the position of the substituent as well as the

Table 3
Summary of CHARMm calculation of energies (kJ mol^{-1}) and dihedral angles of THIs **4b**,**e**,**k**,**c**,**f**,**l** and their corresponding betaines **3b**,**e**,**k**,**c**,**f**,**l**

4/3	R	Position	Energy	$C_{37}C_{38}C_{14}N_1$ (θ_1)	$C_{14}N_{15}C_{16}C_1$ (θ_2)	$N_{15}C_{16}C_{17}C_4$ (θ_3)
4a	H	–, THI	58.1	–	–	–
3a	H	–, betaine *cisoid*	47.3/49.2	–	17.8/−176.8	55.4/74.5
3a	H	–, betaine *transoid*	45.8/47.9	–	28.2/−156.0	−130.6/−132.8
4b	NO_2	*o*, THI	73.6/81.6	8.8/169.8	–	–
4c	NO_2	*m*, THI	61.5/61.8	12.5/−165.4	–	–
3b	NO_2	*o*, betaine *cisoid*	55.7–59.9	68/−115	24/−176	56/73
3c	NO_2	*m*, betaine *cisoid*	50.7–53.9	60/−119	18/−178	54/74
3b	NO_2	*o*, betaine *transoid*	55.6–60.3	66/−113	35/−154	−129
3c	NO_2	*m*, betaine *transoid*	49.4–52.8	58/−118	27/−155	−131
4e	CH_3	*o*, THI	68.3/71.9	5.2/−136.3	–	–
4f	CH_3	*m*, THI	56.9/57.3	13.3/−165.1	–	–
3e	CH_3	*o*, betaine *cisoid*	45.3–49.1	58/−114	20/−175	56/75
3f	CH_3	*m*, betaine *cisoid*	46.1–48.1	60/−115	19/−179	55/74
3e	CH_3	*o*, betaine *transoid*	44.1/−47.9	67/−117	30/−158	−122/−133
3f	CH_3	*m*, betaine *transoid*	44.6–47.0	58/−116	27/−156	−121/−131
4k	Cl	*o*, THI	72.0/76.4	8.9/−165.1	–	–
41	Cl	*m*, THI	57.7/58.0	12.9/−165.5	–	–
3k	Cl	*o*, betaine *cisoid*	45.8–50.6	59/−113	20/−179	56/74
3l	Cl	*m*, betaine *cisoid*	47.6–49.8	60/−115	18/180	55.75
3k	Cl	*o*, betaine *transoid*	44.6–49.1	66/−116	29/−157	−123/−132
3l	Cl	*m*, betaine *transoid*	46.3–48.6	58/−114	28/−155	−121/−131

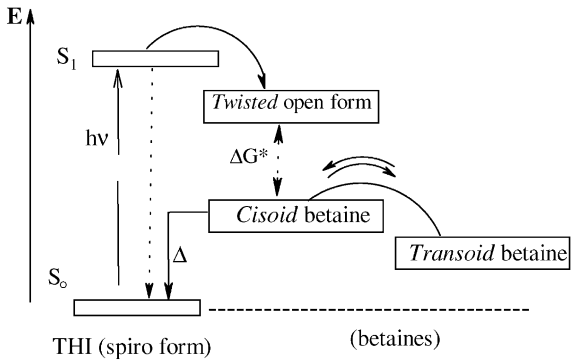

Fig. 19. Proposed energy profile for the formation of betaines **3** (*cisoid* and *transoid* forms) and thermal cyclization to spiro form **4**.

quasi-isoenergetic level of the *cisoid* **3**″ and *transoid* betaine **3**″ indicate that the rate determining step is not the rotation from the *transoid* to the *cisoid* betaine as suggested [23a], but the interconversion of *cisoid* betaine **3**″ to the twisted open form **3**′. The position and size of the groups are of importance only in this step. When one molecule attains this twisted open form **3**′ ring closure should progress easily. Taking into account the above conclusions of the behavior of the THIs **4** and the corresponding *cisoid* **3**″ and *transoid* betaines **3**‴ the energy diagram for the ring closure process can be elucidated (Fig. 19).

4. Conclusions

The steric effect of different substituents in 10′b-phenyl ring of THIs **4** and betaines **3** was proved by CHARMm calculations. The final structure proof was carried out by X-ray analysis of the 10′b-(*o*-iodophenyl) THI **4q**. An interesting aspect of the X-ray structure of **4q** is that the 10′b-(*o*-iodophenyl) ring was found to be under both fluorene core and dihydroisoquinoline, so that the steric effect of 10′-b(*o*-iodophenyl), especially in the presence of the big size iodine atom, with the fluorene skeleton and isoquinoline part is very high, leading to very slow electrocyclization betaine **3q** [17] by UV-irradiation.

The introduction of different groups with various steric demands on the phenyl residue in the 10′b position of the THIs **4** leads to shifting absorption of the ring open betaine and to an exceptional change of half-life of the 1,5-electrocyclization. The presence of the substituents does not greatly influence the maximum of absorption, but the molar extinction coefficient increases with the introduction of different groups. While the groups in *meta*- and *para*-positions have in all the cases the same molar absorption coefficient, the *ortho*-position effects a 20% lower ε value than the *meta*- and *para*-substituted **4**. The rate constant (k) of the 1,5-electrocyclization of the colored betaines **3** → THIs **4** can be decelerated by introducing voluminous substitutents in the *ortho*-position of the phenyl ring. It is generally observed that the electrocyclization of 10′b-(*o*-substituted phenyl)betaines **3b**,**e**,**h**,**k**,**n**,**q** are generally slower by a factor 3 (as in **3h**) to 900 (**3q**) compared to the standard **3a**. A comparison of each *ortho*-substituent to the corresponding *para* showed decrease by factor of 4 for *o*-, *p*-fluoro-substitution **3h**,**j** and factor of 2000 for *o*-, *p*-iodine substitution **3q**,**r**. *Meta*- and *para*-substitution showed no pronounced influence on the half-life which indicates clearly that the steric effect in *ortho*-position hindered 1,5-electrocyclization [17,24–26]. It was notable that an

increase of the atom size in the *ortho*-position, performed by introducing successively halogen atoms from fluorine to iodine, correlates with an enormous increase in half-lives factor 220. By this way the photophysical behavior of the photochromic THIs **4** can be tuned in a directed way.

The steric influence of the different substituents of the *cisoid* **3**″ and *transoid* ring open betaine **3**‴ was analyzed by molecular modeling using CHARMm calculations. The energy content of both forms is found to be independent of the *ortho*- or *meta*-position of the substituent. Furthermore the computations show that there is no obvious hindrance for a rotation which allows the transition between both betaine forms **3**″ and **3**‴. For the computation of the THI **4a**, one structure was found with energy of 58.1 kJ mol^{-1}. Both the structures of THIs **4b**,**e**,**k**,**c**,**f**,**l** have nearly the same energies with an exception of compound **4b**, where the difference of energy amounts to 8 kJ mol^{-1}. It is observed that the ring closed form **4b** (*ortho*) is between 10 and 15 kJ mol^{-1} higher in energy than the corresponding *meta*-position In contrast to the betaines **3**, an important difference of stability between the *ortho*- and *meta*-substituted THI **3** was found. Based on these results we consider that the rate constant of the electrocyclic ring closure is not controlled by the transition *transoid* **3**‴ to *cisoid* **3**″ but by the formation of the twisted open form **3**′ starting from the *cisoid* form **3**″, which undergoes a fast exchange with the *transoid* betaine form **3**‴.

Acknowledgements

The corresponding author is very indebted to Prof. Dr. H. Bouas-Laurent in the Laboratoire de Chimie Organique et Organometallique (LCOO), University of Bordeaux I, France for his kindness, encouragement during his stay in his laboratory. Also, we are grateful to Dr. Christian Weber in Universität des Saarlandes, Saarbrücken, Germany for his assistance with some molecular modeling calculations.

References

[1] H. Dürr, H. Bouas-Laurent (Eds.), Photochromism, Molecules and Systems, Elsevier, Amsterdam, 1990.
[2] J.C. Crano, R.J. Guglielmetti (Eds.), Organic Photochromic and Thermochromic Compounds, vol. I, II, Kluwer Academic Publishers, New York, 1999.
[3] H. Dürr, Pure Appl. Chem. 62 (1990) 1477.
[4] C.B. McArdle (Eds.), Applied Photochromic Polymer Systems, Blackie, New York, 1992.
[5] A.V. El'sov (Eds.), Organic Photochromes, Plenum, New York, 1990.
[6] A. Osuka, D. Fujikane, H. Shinmori, S. Kobatake, M. Irie, J. Org. Chem. 66 (2001) 3913.
[7] (a) M. Irie, Chem. Rev. 100 (2000) 1685 (and references therein);
(b) T. Horii, Y. Abe, R. Nakao, J. Photochem. Photobiol. A 144 (2001) 119;
(c) F. Ortica, P.Levi. Brun, R.J. Gugielmetti, U. Mazzucato, G. Favaro, J. Photochem. Photobiol. A 139 (2001) 133 (and references therein).
[8] (a) T. Matusi, T. Nagata, M. Ozaki, A. Fujii, M. Onada, M. Teraguchi, T. Masuda, K. Yoshino, Synth. Met. 119 (2001) 299;
(b) H. Xie, Z. Liu, X. Huang, J. Guo, Eur. Polym. J. 37 (2001) 497;
(c) Z. Yuxia, L. Zhao, Q. Ling, Z. Jianfen, Z. Jiayun, Eur. Polym. J. 37 (2001) 455;
(d) T. Buruiana, E.C. Buruiana, A. Arinei, I. Grecu, Eur. Polym. J. 37 (2001) 343.
[9] (a) A.V. Tomov, A.I. Voitenkov, Optics Comm. 174 (2000) 133;
(b) L. Angiolini, D. Caretti, L. Giorgini, E. Salatelli, A. Altomare, C. Carlini, R. Solaro, Polymer 41 (2000) 4767;
(c) Y. Aoshima, C. Egami, Y. Kawata, O. Sugihara, M. Tsuchimori, O. Watanabe, H. Fujimura, N. Okamoto, Optics Comm. 165 (1999) 177;
(d) T. Kinoshita, J. Photochem. Photobiol. A 42 (1998) 12;
(e) M. Tanaka, Y. Yonezawa, Mat. Sci. Eng. C4 (1997) 297.
[10] (a) C. Amato, A. Fissi, L. Vaccari, E. Balestrei, O. Pieroni, R. Felicioli, J. Photochem. Photobiol. A 28 (1995) 71;
(b) Y. Wang, H.Q. Yu, Z. T Mu, C.X. Zhao, Z.E.F. Liu, J. Electroanal. Chem. 438 (1997) 127;
(c) P. Ball, C.H. Nichols, Dye Pigment 6 (1985) 13;
(d) S. Shinkai, T. Okawa, Y. Kusano, O. Manabe, K. Kikuwa, T. Goto, T. Matsudo, J. Am. Chem. Soc. 104 (1982) 1960.
[11] (a) J. Labasky, F. Mikes, J. Katal, J. Polm. Bull. 4 (1981) 711;
(b) O. Pieroni, A. Fissi, F. Ciardelli, React. Functional Polym. 26 (1995) 185;
(c) A. Altomare, R. Solaro, L. Angiolini, D. Caretti, C. Carlini, Polymer 36 (1995) 3819.
[12] (a) M. Usui, Y. Shindo, Y. Suzuki, T. Yamagishi, Dye Pigment 30 (1996) 55;
(b) E. Sinkai, O. Manabe, Top. Curr. Chem. 121 (1984) 67;
(c) D. Rötter, H. Rau, J. Photochem. Photobiol. A 101 (1996) 205.
[13] (a) S.A. Ahmed, Th. Hartmann, V. Huch, H. Dürr, A.A. Abdel-Wahab, J. Phys. Org. Chem. 13 (2000) 539;
(b) S.A. Ahmed, A.A. Abdel-Wahab, H. Dürr, Organic Photochemistry and Photobiology, CRC Press, Boca Raton, FL, in press;
(c) Y.S. Tan, S.A. Ahmed, H. Dürr, V. Huch, A.A. Abdel-Wahab, Chem. Commun. 14 (2001) 1246;
(d) R. Fromm, S.A. Ahmed, Th. Hartmann, V. Huch, A.A. Abdel-Wahab, H. Dürr, Eur. J. Org. Chem. 21 (2001) 4077;
(e) S.A. Ahmed, J. Phys. Org. Chem. 15 (2002) 392.
[14] (a) H. Dürr, P. Spang, Angew. Chem. 96 (1984) 277;
(b) H. Bouas-Laurent, H. Dürr, Pure Appl. Chem. 73 (2001) 639;
(c) C. Dorweiler, T. Münzmay, P. Spang, M. Holderbaum, H. Dürr, E. Raabe, C. Kürger, Chem. Ber. 121 (1988) 843;
(d) H. Dürr, C. Schommer, T. Münzamy, Angew. Chem. 98 (1986) 565.
[15] (a) P. Burtscher, H. Dürr, V. Rheinberger, U. Salz, German Pat. DE 195200160 (1995);
(b) H. Dürr, G. Hauck, Deutsche Offenlegungs Schrift Pat. 2906193 (1979);
(c) H. Dürr, H. Gross, K.D. Zils, Deutsche Offenlegungs Schrift Pat. 3220275A1 (1983).
[16] (a) H. Dürr, H.P. Jeonsson, P. Scheidhauer, T. Münzmay, P. Spang, Deutsche Offenlegungs Schrift Pat. 35214325 (1985);
(b) H. Dürr, K.P. Janzen, A. Thome, B. Braun, Deutsche Offenlegungs Schrift Pat. 35214325 (1988);
(c) H. Dürr, H. Gross, K.D. Zils, G. Hauck, H. Hermann, Chem. Ber. 116 (1983) 3915;
(d) Y.S. Tan, Th. Hartmann, V. Huch, H. Dürr, J. Kossanyi, J. Org. Chem. 66 (2001) 1130.
[17] (a) S.A. Ahmed, C. Weber, Z.A. Hozien, Kh.M. Hassan, A.A. Abdel-Wahab, H. Dürr, in preparation;
(b) S.A. Ahmed, Ph.D Thesis, Saarland-Assiut University, 2000.
[18] (a) A. Bischler, B. Napieralski, Berichte. 26 (1893) 1903;
(b) L.F. Tietze, T. Eicher (Eds.), Reaktion und Synthesen, Thieme Verlag, Stuttgart, 1981, p. 319.

[19] F. Ritschie, N.S. Wales, Proc. Roy. Soc. 78 (1945) 147.
[20] W.J.L. Radom, J.A. Pople, J. Am. Chem. Soc. 94 (1972) 1496.
[21] (a) H. Quast, K.H. Roß, E. Spiegel, K. Peters, H.G.V. Schnering, Angew. Chem. 89 (1977) 202;
(b) G. Ege, K. Gilbert, F.W. Nader, Chem. Ber. 114 (1981) 1074;
(c) P. Dorweiler, P. Spang, H. Dürr, K. Peters, H.G.V. Schnering, Isreal. J. Chem. 25 (1983) 241.
[22] (a) A. Thome, Ph.D Thesis, Universität des Saarlands, Saarbrücken, 1987;
(b) P. Spang, Ph.D Thesis, Universität des Saarlandes, Saarbrücken, 1985.
[23] (a) T. Münzamy, Ph.D Thesis, Universität des Saarlands, Saarbrücken, 1986;
(b) T. Münzamy, P. Spang, M. Holderbaum, H. Dürr, E. Raba, C. Krüger, Chem. Ber. 121 (1988) 843.
[24] (a) G.H. Beaven, in: G.W. Gray (Ed.), Steric Effects in Conjugated Systems, Butterworths Sci. Pub., London, 1958, p. 22;
(b) C.C. Barker, in: G.W. Gray (Ed.), Steric Effects in Conjugated Systems, Butterworths Sci. Pub., London, 1958, p. 34;
(c) E.S. Waight, R.L. Erskine, in: G.W. Gray (Ed.), Steric Effects in Conjugated Systems, Butterworths Sci. Pub., London, 1958, p. 73.
[25] (a) P.R. Wells (Ed.), Linear Free Energy Relationships, Academic Press/Prentice-Hall, London/New York, 1968;
(b) G.E.K. Branch, M. Calvin, (Eds.), The Theory of Organic Chemistry, Prentice-Hall, New York, 1941, p. 443;
(c) L.P. Hammett, J. Am. Chem. Soc. 59 (1937) 96;
(d) L.P. Hammett (Ed.), Physical Organic Chemistry, McGraw-Hill, New York, 1940, p. 184.
[26] (a) N.R. Chapman, J. Shorter (Eds.), Correlation Analysis in Chemistry, Plenum Press, New York, 1978;
(b) S. Wold, M. Sjöström, in: N.B. Chapman, J. Shorter (Eds.), Correlation Analysis in Chemistry, Plenum Press, New York, 1978;
(c) O.L. Davis, P.L. Goldsmith (Eds.), Statistical Methods in Research and Production, Oliver & Boyd, Edinburgh, 1972.
[27] A.W. Hofmann, Berichte. 5 (1872) 713.
[28] (a) C. Andreis, H. Dürr, V. Wintgens, P. Valat, J. Kossanyi, Chem. Eur. J. 3 (1997) 509;
(b) C. Andreis, Ph.D Thesis, Universiteat des Saarlandes, Saarbrücken, 1996;
(c) H. Bleisinger, P. Scheidhauer, H. Dürr, V. Wintgens, P. Valat, J. Kossanyi, J. Org. Chem. 63 (1998) 990.